Quantum theory of the dynamical Čerenkov emission of x rays

Ariel Caticha*

National Institute of Standards and Technology, Gaithersburg, Maryland 20899
and Institute for Physical Science and Technology, University of Maryland, College Park, Maryland 20742
(Received 10 April 1991; revised manuscript received 30 October 1991)

X-ray photons propagating in a crystal close to the Bragg-diffraction directions have an effective index of refraction that may be larger than 1. Electrons moving rapidly in crystals may therefore emit x rays. This process, the dynamical Čerenkov radiation (DCR) of x rays, is studied with use of a theory that is closely analogous to the quantum theory of the Čerenkov effect in homogeneous media. Features of the DCR process that are calculated include the spectral width due to x-ray absorption, the systematic deviations of the photon energy from Bragg's law, the influence of the orientation of the crystal surface, etc. Extensions of the theory to cover many-beam diffraction cases or more detailed calculations of the small recoil effects are straightforward to carry out. The photons are emitted at the far tails of the diffraction region, they are overwhelmingly in the "diffracted" plane-wave component, and, in the two-beam case there is no anomalous Borrmann absorption. DCR is a particularly efficient emission process for hard x rays (several tens of keV) with extremely high spectral density (within small angular regions). The emission rate is highest at the energy $\hbar\omega = \gamma\hbar\omega_p$ (ω_p is the plasma frequency), but, because of absorption, the number of photons that actually emerge from the crystal will peak at appreciably higher energies. The production of photons of a given energy is optimized by using lattice planes with the lowest possible Miller indices and by asymmetrically cutting the crystal surface. The use of DCR for a tunable source of hard x rays should therefore be seriously considered.

I. INTRODUCTION

The Čerenkov emission of photons by fast electrons moving in a homogeneous dielectric medium occurs whenever the velocity of the electrons exceeds the phase velocity of the photons. Čerenkov x rays may therefore be emitted only in the very narrow spectral regions of anomalous dispersion; otherwise, the index of refraction is less than 1 and the process is forbidden. In a periodic medium, however, the situation changes. According to classical theories originally developed by Garibyan and Yang[1] and also by Baryshevsky and Feranchuk,[2] when a charged particle moves rapidly through a crystal, intense and sharp x ray beams are emitted in the close vicinity of the Bragg directions. This emission was originally interpreted as being due to the diffraction of the electromagnetic field associated to the electron, but later it was realized that it could be due to a kind of Čerenkov effect.[3] In fact, according to the dynamical theory of x-ray diffraction (DTXD),[4] x-ray photons propagating in a crystal close to the Bragg directions experience an effective index of refraction, $n_d = ck/\omega$ (where $\hbar k$ is the crystal momentum) which may indeed be larger than one. A quantum theory of this dynamical Čerenkov radiation

(DCR), which is also known under various other names such as dynamic radiation, parametric x rays, and quasi-Čerenkov radiation, has been given by Baryshevsky and Feranchuk[5] for the special case in which the electrons are normally incident to the crystal surface.

The classical theory of this phenomenon was more recently extended[6] to include situations of oblique electron incidence and also to include situations where the Bragg angle θ_B may be close to $\pi/2$ for which some of the usual approximations are known to fail.[7,8] More importantly, it was shown that, very close to the DCR beam, there is another beam which tends (for electron energies of a few hundred MeV) to be less intense and much broader both angularly and spectrally than the DCR beam. It is this beam which is to be interpreted as being due to the dynamical diffraction of the electromagnetic field associated to the electron and was dubbed the "transition-diffracted" beam (TDR).

In the last few years a number of the broader features of these phenomena seem to have been experimentally confirmed[9–13] but detailed verifications have not yet been carried out. In this paper a quantum theory of the dynamical Čerenkov emission of x rays in a crystal is developed in which the formal similarity to the optical

Čerenkov effect in homogeneous media is preserved and exploited. The quantum theory of the Čerenkov emission of optical photons is normally developed within the context of a phenomenological quantum electrodynamics[14] in which the medium is described by a linear (possibly anisotropic) uniform dielectric susceptibility χ. The present work is based on an extension of such a phenomenological quantum electrodynamics to x rays[15] for which a nonuniform periodic susceptibility $\chi(\mathbf{r})$ must be used.

A very important difference between our approach and that of Baryshevsky and Feranchuk[5] lies in their use of photon-wave fields which involve asymptotically incoming spherical waves and outgoing plane waves to take into account the finite crystal size as well as dynamical diffraction and absorption effects. Such wave fields are necessarily complicated. In contrast, we find that one is not required to simultaneously include the effects of x-ray absorption and of the finite crystal size from the very start. They can be correctly included after the main features of DCR process in an infinite nonabsorbing crystal have been elucidated. This procedure has the advantage of making the physics more transparent. One can clearly separate the DCR features that are inherent to the DCR process itself, from those due to absorption, and from those which are traceable to the existence and orientation of the boundaries. Among other things, we may calculate the effects of the recoil of the electron, the deviation of the photon energy from a naive Bragg's-law prediction, the effect of non-normal electron incidence on an asymmetrically cut crystal surface, and the intrinsic spectral width of this emission process.

In Sec. II we review the description of the x-ray photon according to the two-beam approximation of the DTXD. The basic DCR emission process in an unbounded nonabsorbing crystal is studied in Sec. III. The effects of absorption and of possibly asymmetrically cut crystal surfaces are then included in Sec. IV. Then, in Sec. V, explicit numerical calculations for a diamond crystal are given. In Sec. VI we summarize our conclusions.

II. THE X-RAY PHOTON

In the dynamical theory of x-ray diffraction,[4] the crystal is described by a periodic dielectric susceptibility,

$$\chi(\mathbf{r}) = \sum_H \chi_H \exp(i\mathbf{H}\cdot\mathbf{r}) , \qquad (2.1)$$

where $\mathbf{H}$ are the reciprocal-lattice vectors, and the x-ray photons are described by Bloch waves

$$A_k^\mu(\mathbf{r},t) = \sum_H A_H^\mu \exp[i(-\omega t + \mathbf{k}_H \cdot \mathbf{r})] , \qquad (2.2)$$

where $\hbar\mathbf{k}$ is the crystal momentum and $\mathbf{k}_H = \mathbf{k} + \mathbf{H}$. The scalar potential A^0 is small, of order χ, and may be neglected.[15] This is in accordance with the main approximation of the DTXD of neglecting terms of $O(\chi^2)$ in phases and terms of $O(\chi)$ in the amplitudes.

It is convenient to define the so-called resonance defects ξ_0 and ξ_H by

$$\mathbf{k}^2 = K^2(1 + \chi_0 + 2\xi_0) \qquad (2.3)$$

and

$$\mathbf{k}_H^2 = K^2(1 + \chi_0 + 2\xi_H) , \qquad (2.4)$$

where $K = \omega/c$. Thus, the effective index of refraction n_d, which is given by

$$n_d = \frac{ck}{\omega} = 1 + \frac{\chi_0}{2} + \xi_0 , \qquad (2.5)$$

contains a contribution $\chi_0/2$ which is usually negative and a dynamical diffraction contribution ξ_0, which, in situations where DCR occurs, is positive and dominant (see Fig. 1).

In the two-beam case, the two wave vectors $\mathbf{k}$ and $\mathbf{k}_H$ are constrained to lie on the dispersion surface shown in Fig. 1 and given by

$$\xi_0\xi_H = \frac{x^2}{4} , \qquad (2.6)$$

where $x = (\chi_H\chi_{-H}P^2)^{1/2}$ and P, the polarization factor, is either 1 or $\cos(2\theta)$ (where θ is the angle between $\mathbf{k}$ and $\mathbf{H}$) depending on whether we deal with a ϕ or a θ polarization ($\mathbf{A}_0$ perpendicular or parallel to the plane defined by $\mathbf{k}$ and $\mathbf{H}$), respectively.

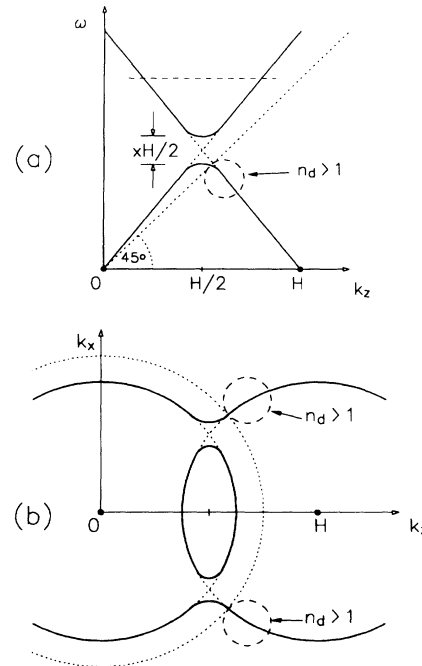The amplitude ratio $R = A_H/A_0$ is given by

FIG. 1. The dispersion surface for x-rays in a two-beam case showing how the dynamical contribution ξ_0 in Eq. (2.5) may lead to Bloch photon states lying outside the vacuum lightcone. These photons, for which $n_d > 1$, are the ones emitted in the DCR process. Shown are projections of the dispersion surface into (a) the ω-k_z plane and (b) the ω=const and k_y=const surface represented by the dashed line in (a). The splittings of the dispersion surface are small, proportional to $x = (\chi_H\chi_{-H}P^2)^{1/2}$.

$$R \equiv \frac{A_H}{A_0} = \frac{2\xi_0}{P\chi_{-H}} = \frac{P\chi_H}{2\xi_H} . \tag{2.7}$$

In Fig. 1 we notice that the condition for DCR emission is only satisfied at the tails of the diffraction region. It is easy to see that this follows from the generally valid relation $|\chi_0| > |\chi_H|$. This feature of DCR has a number of interesting implications. For example, the amplitude ratio R of the emitted photons tends to be rather large[4] and the photons are therefore mostly in the diffracted wave. Also, the DCR photons should not appreciably exhibit those dynamical diffraction effects such as the Borrmann effect which depend on the interference between the primary and the diffracted beams because the two beams are of quite different amplitudes. This will be discussed further later.

Normally the experimental setup is such that it is convenient to express ξ_0 in terms of the fixed frequency and angle of incidence of an externally generated incident beam. In the present situation one is interested in x rays generated inside the crystal and it turns out to be more convenient to express ξ_0 in terms of the wave vector $\mathbf{k}$. Then[16]

$$\xi_0 = \frac{x}{2} [-\Upsilon \pm (\Upsilon^2 + 1)^{1/2}] , \tag{2.8}$$

where $\pm$ refer to the two branches of the dispersion surface and where

$$\Upsilon = \frac{2\mathbf{k} \cdot \mathbf{H} + H^2}{2xk^2} . \tag{2.9}$$

The diffraction region is centered around $\Upsilon \simeq 0$. It is easy to see that the DCR photons lie in the branch of the dispersion surface corresponding to the $+$ sign in Eq. (2.8).

In the absence of absorption one may always choose the origin so that, for a given single family of planes $\mathbf{H}$, one may write $\chi_{-H} = \chi_H$. For centrosymmetric crystals this can be done for all $\mathbf{H}$ simultaneously even in the presence of absorption. In what follows we will therefore take $\chi_{-H} = \chi_H$.

In the Coulomb gauge, $\nabla \cdot \mathbf{A} = 0$, the amplitudes $\mathbf{A}_H$ may be normalized to one photon $\hbar\omega_k$ per volume V according to[15]

$$\sum_H \mathbf{k}_H^2 \mathbf{A}_H \cdot \mathbf{A}_H^* = \frac{\hbar\omega_k}{2V} . \tag{2.10}$$

This implies that, in the two-beam approximation,

$$A_0 \simeq \left[\frac{\hbar c^2}{2\omega V} \frac{1}{1+|R|^2} \right]^{1/2} , \tag{2.11}$$

which, for $R=0$ reduces to the conventional vacuum normalization.

III. DYNAMICAL ČERENKOV RADIATION IN AN UNBOUNDED, NONABSORBING CRYSTAL

A. General expression for the emission rate

Let us consider an electron which is moving sufficiently fast ($\gamma = E/mc^2$ of the order of 10^2 or more) in a crystal of sufficiently light atoms (say, carbon or silicon). It is a reasonably good approximation to neglect the multiple scatterings of the electron and to use the plane-wave solutions of the free Dirac equation to describe its motion. Then the rate of photon emission in an unbounded nonabsorbing crystal is calculated in a straightforward way using the golden rule. After averaging over the initial spins and summing over the final spins of the electron,[17] the result for the number of photons of a given polarization emitted per unit time into a given region $\mathcal{H}$ of photon states by an electron of momentum $\mathbf{p}$ is

$$\frac{dN}{dt} = \sum_{\mathbf{k} \in \mathcal{H}} \frac{2\pi e^2}{\hbar} \sum_H \delta(E - E_F - \hbar\omega) S_H (N_k + 1) , \tag{3.1}$$

where $E = E(\mathbf{p}) = (c^2 \mathbf{p}^2 + m^2 c^4)^{1/2}$ and $E_F = E(\mathbf{p} - \hbar\mathbf{k})$. N_k is the number of photons already present in mode $\mathbf{k}$, and (neglecting the scalar potentials, which are of order χ) (Ref. 15)

$$S_H = \frac{1}{1-\hbar\omega/E} \left[|\beta \mathbf{A}_H \cdot \hat{\mathbf{p}}|^2 + \mathbf{A}_H \cdot \mathbf{A}_H^* \right.$$
$$\left. \times \left[\frac{\beta c \hbar \mathbf{k} \cdot \hat{\mathbf{p}}}{\hbar\omega} - 1 \right] \frac{\hbar\omega}{E} \right] , \tag{3.2}$$

where $\beta = (1 - \gamma^{-2})^{1/2}$ and where the caret is used to denote unit vectors. Neglecting recoil, this takes the simple form

$$S_H = |\beta \mathbf{A}_H \cdot \hat{\mathbf{p}}|^2 . \tag{3.3}$$

For very hard x rays, with very small Bragg angles, $k \gg O(H)$, more than one reciprocal-lattice vector may simultaneously contribute in the sum over $\mathbf{H}$ in Eq. (3.1). This will doubtless give rise to interesting interference effects. From now on, however, we will restrict ourselves to the simpler situation in which only one term in the sum over $\mathbf{H}$ gives a nonzero contribution to the emission rate. We may then relabel the single contributing component $\mathbf{A}_H$ of the Bloch wave by $\mathbf{A}_0$. Then

$$\frac{dN}{dt} = \sum_{\mathbf{k} \in \mathcal{H}} \frac{2\pi e^2}{\hbar} \delta(E - E_F - \hbar\omega_k) S_0 (N_k + 1) . \tag{3.4}$$

Equation (3.4) is the expression we wanted for the emission rate. It includes both spontaneous and stimulated emission. If we put $\hbar\omega = \hbar ck/n$ and $R=0$, it reduces to the quantum Čerenkov emission rate of optical photons[14] and if, furthermore, the recoil terms are neglected (which is equivalent to taking $\hbar \to 0$), the spontaneous emission rate gives the classical result of Frank and Tamm.[18]

B. The direction and energy of the emitted photon

The condition that the argument of the δ function in Eq. (3.4) vanishes can be written in the form

$$\frac{1}{n_d} - \beta \hat{\mathbf{k}} \cdot \hat{\mathbf{p}} = \frac{\hbar c k}{2E} \left[\frac{1}{n_d^2} - 1 \right] , \qquad (3.5)$$

which is precisely the condition for Čerenkov emission including recoil effects.[19] Neglecting recoil, and for a nondispersive optical index of refraction n, (3.5) is the equation for the Čerenkov cone. In the x ray case, n_d is highly dispersive and anisotropic and the usual cone structure is lost.

Since DCR originates in an effective index of refraction due to dynamical diffraction, the energy $\hbar\omega_C$ of the emitted photon necessarily lies close to that determined by Bragg's law. Let

$$\hbar\omega_C = \hbar\omega_B(1 + \epsilon_C) , \qquad (3.6)$$

where

$$\hbar\omega_B \equiv \frac{\hbar c H}{2\cos\theta} , \qquad (3.7)$$

and $\cos\theta = -\hat{\mathbf{k}} \cdot \hat{\mathbf{H}}$. To calculate the correction ϵ_C, we first calculate the resonance defect ξ_{0C} of the emitted photon using Eqs. (2.5) and (3.5):

$$\xi_{0C} = \frac{1 - \beta \hat{\mathbf{k}} \cdot \hat{\mathbf{p}}}{1 - r} - \frac{\chi_0}{2} , \qquad (3.8)$$

where $r = \hbar\omega_B / E$ introduces a small recoil correction. The fact that this solution for ξ_{0C} exists independently of the electron energy means that, in contrast to the optical Čerenkov effect, there is no sharp energy threshold below which DCR will not occur. This important feature of the DCR process is already well known. If one neglects recoil, ξ_{0C} takes the simple form

$$\xi_{0C} \simeq \frac{1}{2}(\gamma^{-2} - \chi_0 + \psi^2) , \qquad (3.9)$$

where ψ is the angle between $\mathbf{k}$ and $\mathbf{p}$. Substituting into Eqs. (2.7) and (2.8), one obtains expressions for the amplitude ratio R and the auxiliary variable Υ:

$$R_C = \frac{2\xi_{0C}}{P\chi_{-H}} \qquad (3.10)$$

and

$$\Upsilon_C = \frac{1}{2} \left[\frac{x}{2\xi_{0C}} - \frac{2\xi_{0C}}{x} \right] . \qquad (3.11)$$

The energy correction ϵ_C is then obtained from (2.5) and (2.9):

$$\epsilon_C = -\frac{1}{2} \left[\frac{x\Upsilon_C}{\cos^2\theta} + \chi_0 + 2\xi_{0C} \right] . \qquad (3.12)$$

We saw in Sec. II that a number of very interesting consequences follow from the fact that DCR occurs at the edge of the diffraction region where $|R_C|$ tends to be rather large. A more quantitative argument is as follows:

DCR cannot occur for $n_d < 1$ and this sets an absolute minimum value for R. From (2.5) and (2.7) we get

$$|R_{\min}| = \left| \frac{\chi_0}{P\chi_H} \right| > 1 .$$

Actually, the least values for $|R_{\min}|$ (obtained for strong reflections, χ_H large such as say, diamond 111) give $R_{\min} \sim -3$ and $\Upsilon \sim -5$. Since appreciable diffraction and Borrmann effect occur[4] for $|\Upsilon|^2 < 1$, this shows that emission occurs in the tails of the diffraction region, that there is negligible anomalous absorption, etc.

We now consider two more implications of this fact. Neglecting quantities of order $|R_C^{-2}|$ relative to quantities of order 1 (at the very worst this is accurate to 10%, and more typically to a fraction of 1% or less) and using (3.9), it follows that the already small ϵ_C may be approximated by

$$\epsilon_C \simeq \frac{1}{2} \left[\frac{\gamma^{-2} + \psi^2 - \chi_0}{2\cos^2\theta} - \gamma^{-2} - \psi^2 \right] . \qquad (3.13)$$

From this equation one sees, first, that the small correction ϵ_C depends on the electron energy, at least up to values of γ of the order of $|\chi_0|^{-1/2}$, and second, that photons of different polarizations emitted at the same $\hat{\mathbf{k}}$ will have approximately the same energy.

Since the photon is very nearly a plane wave propagating in the direction of the diffracted beam $\mathbf{k}_H = \mathbf{k} + \mathbf{H}$, it is important to determine the direction of $\mathbf{k}_H$ relative to $\mathbf{H}$. Using Eq. (2.9), one finds $\cos\theta_H$ to be given by

$$\cos\theta_H = \cos\theta \, (1 + x\Upsilon_C \tan^2\theta) . \qquad (3.14)$$

To summarize our results up to this point: the similarities [i.e., Eqs. (3.4) and (3.5)] with the optical Čerenkov effect can be made explicit and exploited to simplify the treatment of DCR. This is done by expressing the various quantities of interest in terms of the "primary" wave vector $\mathbf{k}$ even though the photon exists mostly in the "diffracted" component $\mathbf{k}_H$. It is then a simple matter to calculate the energy $\hbar\omega$ and direction of propagation of the photon.

C. The spontaneous emission rate

For sufficiently large volume V, the sum over $\mathbf{k}$ in (3.4) may be replaced by an integral over $d^3k = k^2 dk \, d\Omega$. The δ function makes the integration over dk straightforward. Thus, to leading order in χ and in r [i.e., using (3.3)], the number of photons of polarization $\hat{\mathbf{e}}$ radiated per unit time with $\hat{\mathbf{k}}$ within $d\Omega$ is

$$\frac{dN}{dt \, d\Omega} = \frac{\alpha}{8\pi} \frac{cH}{\cos^3\theta} \frac{|\hat{\mathbf{e}} \cdot \hat{\mathbf{p}}|^2}{|R_C|^2} , \qquad (3.15)$$

where $\alpha = \frac{1}{137}$. Substituting (3.9) and (3.10), this may be written in the simple form

$$\frac{dN}{dt \, d\Omega} = \frac{\alpha}{8\pi} \frac{cH}{\cos^3\theta} \left[\frac{\hat{\mathbf{e}} \cdot \hat{\mathbf{p}} \, x\psi_m^{-2}}{1 + (\psi/\psi_m)^2} \right]^2 , \qquad (3.16)$$

where

$$\psi_m = (\gamma^{-2} - \chi_0)^{1/2} \ . \tag{3.17}$$

Except for the slowly varying $\cos^{-3}\theta$ factor, the angular dependence in (3.16) is given by the factor in parentheses. Roughly, the emission rate is maximum for $\hat{k}$ in a cone forming an angle ψ_m with $\hat{p}$. Notice that this differs from the angle $1/\gamma$ typical of other radiation processes by relativistic electrons. To be more precise, let us introduce spherical coordinates (θ, ϕ) with H lying along the z axis, $H = H\hat{e}_z$, and the electron incident along $(\theta_e, \phi_e = 0)$:

$$\hat{p} = \sin\theta_e \hat{e}_x - \cos\theta_e \hat{e}_z \ ,$$

$$\hat{k} = \sin\theta \cos\phi \ \hat{e}_x + \sin\theta \sin\phi \ \hat{e}_y - \cos\theta \ \hat{e}_z \ ,$$

$$\cos\psi = \sin\theta_e \sin\theta \cos\phi + \cos\theta_e \cos\theta \ , \tag{3.18}$$

$$\hat{e}_\theta \cdot \hat{p} = -\sin\theta_e \cos\theta \cos\phi + \cos\theta_e \sin\theta \ ,$$

and

$$\hat{e}_\phi \cdot \hat{p} = -\sin\theta_e \sin\phi \ .$$

Thus, on the plane of incidence $\phi = 0$ the radiation is purely in the θ polarization, while if one varies ϕ at constant $\theta = \theta_e$, the radiation is almost purely ϕ polarized. To be specific let us consider this latter case in more detail. The emission rate is

$$\frac{d^2N_\phi}{dt\,d\Omega} = \left[\frac{d^2N_\phi}{dt\,d\Omega} \right]_{\text{peak}} \left[\frac{2\psi/\psi_m}{1+(\psi/\psi_m)^2} \right]^2 \ . \tag{3.19}$$

This becomes maximum at $\psi = \psi_m$, i.e., at $\phi \simeq \psi_m/\sin\theta_e$ and the peak value is

$$\left[\frac{d^2N_\phi}{dt\,d\Omega} \right]_{\text{peak}} = \frac{\alpha}{8\pi} \frac{cHx^2\psi_m^{-2}}{4\cos^3\theta_e} \ . \tag{3.20}$$

Notice that the peak emission rate depends on the electron energy through ψ_m. For fixed θ_e, raising γ increases the emission rate and tightens the emission "cone" until γ values of the order of $|\chi_0|^{-1/2}$ are reached. After that, saturation occurs and a limiting value is approached.

It is also important to study how the emission rate varies with the electron angle of incidence θ_e. This requires taking into account the dependence of the susceptibility with the photon energy,

$$\hbar\omega_C \simeq \hbar\omega_B = \frac{\hbar cH}{2\cos\theta_e} \ . \tag{3.21}$$

For our purposes it is accurate enough to take

$$\chi_0 = -\frac{\omega_p^2}{\omega_C^2}$$

and

$$\chi_H = -\frac{\omega_p^2}{\omega_C^2} r_F \ , \tag{3.22}$$

where ω_p is the plasma frequency of the medium, r_F is the ratio of the structure factors, $r_F = F_H/F_0$. Then

$$\left[\frac{d^2N_\phi}{dt\,d\Omega} \right]_{\text{peak}} = \frac{\alpha}{8\pi} \left[\frac{\omega_p^2 r_F}{cH} \right]^2 \frac{\gamma}{\omega_p} \left[\frac{2\gamma\omega_p/\omega_C}{1+(\gamma\omega_p/\omega_C)^2} \right] \ . \tag{3.23}$$

This is important: as θ_e is increased towards more grazing incidence (thereby increasing the photon energy), the factor in parenthesis increases towards a maximum. The energy of the photons which are most efficiently radiated is given by

$$\hbar\omega_C = \gamma\hbar\omega_p \ . \tag{3.24}$$

As the angle θ_e is further increased towards 90°, the emission rate drops, vanishing linearly in $\cos\theta_e$. Notice that the apparent singularity $\cos^{-3}\theta$ in Eq. (3.15) has disappeared. The maximum value of the peak emission rate is

$$\left[\frac{d^2N_\phi}{dt\,d\Omega} \right]_{\text{peak}}^{\text{max}} = \frac{\alpha}{8\pi} \left[\frac{r_F}{cH} \right]^2 \gamma\omega_p^3 \ . \tag{3.25}$$

This is proportional to γ. We mentioned earlier that the emission rate for a fixed θ_e saturates as γ increases; we see now that this convergence is nonuniform in θ_e. As γ increases, the maximum peak emission rate occurs for higher incidence angles and at correspondingly higher photon energies.

At this point two comments may be made, first on the influence of the particular family of planes involved in the diffraction process, and second, on the influence of the crystal temperature. Notice that, while the photon energy at which the electron radiates most efficiently, Eq. (3.24), does not depend on the particular family of planes considered, the actual emission rate (3.23) depends rather strongly on H. The emission from lattice planes with low Miller indices will be stronger both because of the larger lattice spacing ($H = 2\pi/d$) and also because of the larger values of the ratio r_F. Since it is the square of these quantities that enters (3.23), their effect is very considerable. Therefore, to produce photons of a given energy there is a marked advantage in using planes with the lowest possible Miller indices at more grazing incidence angles.

The temperature of the crystal affects the DCR process in two ways: changes in the interplanar spacing produce shifts of the emitted photon energy which are directly calculable from Eq. (3.6), and second, the Fourier components χ_H of the susceptibility are altered through the Debye-Waller factor. To increase the emission rate one would, again, use planes with the lowest possible Miller indices, at temperatures well below the Debye temperature.

IV. THE EFFECTS OF X-RAY ABSORPTION

X-ray absorption has two main effects on the DCR process: first, not all the emitted photons manage to leave the crystal, and second, the photons emitted in a given direction do not have a sharply defined energy but acquire a Lorentzian line shape. From an experimental point of view the angle that is directly observable is the angle θ_R which the emitted x rays make with H after they leave the crystal. It involves small refraction correc-

tions which are easy to calculate:

$$\cos\theta_R = \cos\theta \left[1 + x\Upsilon_C \tan^2\theta + \frac{\chi_0}{2}\right] - \frac{\chi_{0r}\hat{\mathbf{n}}\cdot\hat{\mathbf{e}}_z}{2\cos\theta} \ . \qquad (4.1)$$

As remarked earlier, the DCR photons will suffer absorption in the medium given by the usual, non-Borrmann, linear absorption coefficient μ_0. This justifies the following simple considerations. The total number of photons which actually reaches the crystal surface is obtained by integrating the emission rate multiplied by the appropriate absorption factor over the time the electron takes to traverse the medium. For a crystal slab of thickness l bounded by plane and parallel surfaces, the normal to which is $\hat{\mathbf{n}}$, one obtains

$$\frac{dN}{d\Omega_R} = \left|\frac{\hat{\mathbf{n}}\cdot\hat{\mathbf{k}}_R}{\hat{\mathbf{n}}\cdot\hat{\mathbf{v}}}\right| \left[1 - \exp\left[-\frac{\mu_0 l}{\hat{\mathbf{n}}\cdot\hat{\mathbf{k}}_H}\right]\right] \frac{1}{\mu_0 v}\frac{dN}{dt\,d\Omega} \ . \qquad (4.2)$$

This same expression holds irrespective of whether the photon beam exits the crystal by the surface through which the electron entered (Bragg case) or left it (Laue case). One sees that larger intensities should be observed if the crystal surface is cut so that the electrons enter tangentially to it. The reason for this is that most photons are produced closer to the surface and experience smaller absorption. For extreme cases of $\hat{\mathbf{n}}\cdot\hat{\mathbf{v}}\rightarrow 0$, however, Eq. (4.2) ceases to be valid. In this situation neither the multiple scatterings of the electron nor the reflection of the photon at the surface should be neglected.

For thick crystals one obtains the following simple expression:

$$\frac{dN}{d\Omega_R} = \left|\frac{\hat{\mathbf{n}}\cdot\hat{\mathbf{k}}_R}{\hat{\mathbf{n}}\cdot\hat{\mathbf{v}}}\right| \tau \frac{d^2N}{dt\,d\Omega} \ . \qquad (4.3)$$

where $1/\mu_0 v \simeq \tau$ is the photon "lifetime."

So far, the photons emitted in a given direction have been considered to be sharply defined in energy with $\hbar\omega_C$ given by Eq. (3.6). Absorption causes them to have a finite width W with a Lorentzian distribution

$$\frac{W/2\pi}{(\hbar\omega - \hbar\omega_C)^2 + W^2/4} \ . \qquad (4.4)$$

From Eqs. (3.6) and (3.13) we see that the presence of absorption leads to an imaginary part for the photon energy. This imaginary part translates into the width

$$W = \frac{\hbar\omega_B \chi_{0i}}{2\cos^2\theta} = \frac{1}{2\cos^2\theta}\frac{\hbar}{\tau} \ . \qquad (4.5)$$

The presence of χ_{0i} in (4.5), without any dynamical Borrmann corrections, is again a reflection of the fact that DCR occurs at the very tails of the diffraction region.

Experimentally one wants the externally measured $d^2N/d\hbar\omega\,d\Omega_R$ instead of $d^2N/d\hbar\omega\,d\Omega$. In the former expression, the angle θ_R is varied at constant $\hbar\omega$. This means the wave vector $\mathbf{k}$ is constrained to move on the plane defined by Eq. (3.5). It follows then that

$$d\theta \simeq \hat{\mathbf{p}}\cdot\hat{\mathbf{k}}\left|\frac{\hat{\mathbf{n}}\cdot\hat{\mathbf{k}}_R}{\hat{\mathbf{n}}\cdot\hat{\mathbf{v}}}\right| d\theta_R \ , \qquad (4.6)$$

so that

$$\frac{d^2N}{d\hbar\omega\,d\Omega_R} \simeq \left|\frac{\hat{\mathbf{n}}\cdot\hat{\mathbf{k}}_R}{\hat{\mathbf{n}}\cdot\hat{\mathbf{v}}}\right| \frac{dN}{d\Omega_R}\frac{W/2\pi}{(\hbar\omega - \hbar\omega_C)^2 + W^2/4} \ . \qquad (4.7)$$

This expression agrees with the expression derived classically in Ref. 6. That this is not immediately obvious is due to differences of notation and to the fact that the classical expression describes not just DCR but also the transition-diffracted beam. Notice that the asymmetry factor $|\hat{\mathbf{n}}\cdot\hat{\mathbf{k}}_R/\hat{\mathbf{n}}\cdot\hat{\mathbf{v}}|$ appears squared: one of these factors is connected to the effective absorption paths while the other is analogous to the asymmetry factor $b^{-1} = \hat{\mathbf{n}}\cdot\mathbf{K}_H/\hat{\mathbf{n}}\cdot\mathbf{K}_0$ familiar from the DTXD.

V. AN EXAMPLE

In this section we calculate the DCR emitted by an electron as it moves in a diamond crystal. To be specific we will consider only the (111) diffracting planes. In diamond, these planes are responsible for the most intense reflections. We will consider the symmetric case with the crystal surface cut parallel to the (111) planes. These restrictions are, of course, not essential. The treatment of the previous sections is of more general validity.

In Fig. 2 we show the number of photons per steradian which exits the crystal, given by Eq. (4.3), in the plane of incidence ($\phi = 0$), by an electron of energy $\gamma = 300$ (about 150 MeV) as it moves at an angle of 85° to the (111) direction. Bragg's law gives energies for these photons around 35 keV. The factor $\hat{\mathbf{e}}\cdot\hat{\mathbf{p}}$ in the emission rate implies that these photons are totally polarized in the θ direction. One recognizes this emission pattern as a section of the "cone" of opening angle $2\psi_m$. The angle $\psi_m \simeq 3.51$ mrad,
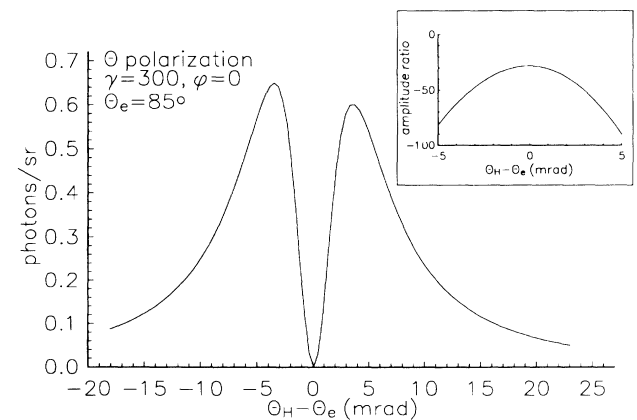
FIG. 2. The number of photons per steradian which exits the crystal as a function of the emission angle, in the plane of incidence ($\phi = 0$), emitted by an electron of energy $\gamma = 300$ as it moves at an angle of 85° to the (111) direction. Inset: the amplitude ratio for the central portion of the emission pattern showing that the relevant values of R_c are rather large.
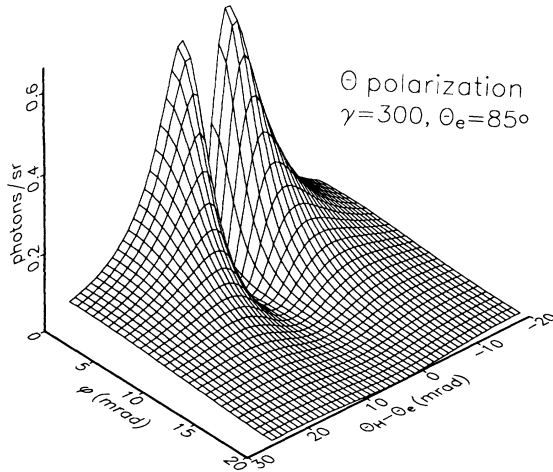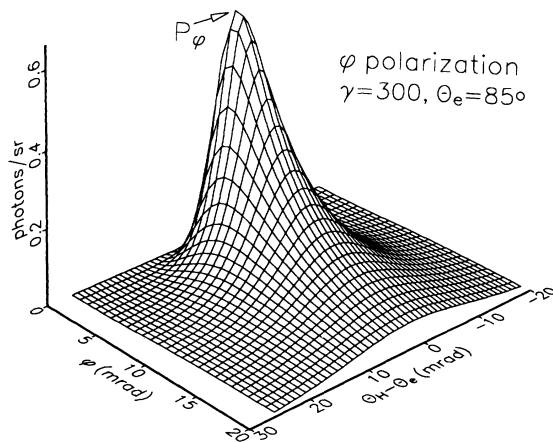
FIG. 3. The number of photons per steradian which exits the crystal as a function of the emission direction (θ polarization, $\gamma = 300$, $\theta_e = 85°$).
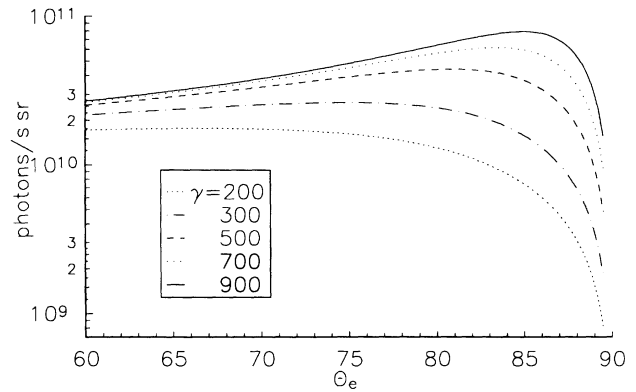

FIG. 5. The peak of the ϕ-polarization emission rate (photons per steradian per s), which occurs at the point P_ϕ in Fig. 4, is plotted against the angle of incidence of the electron θ_e for several electron energies.

is close to, but definitely different from, $1/\gamma \simeq 3.33$ mrad. The peak at higher angles is less intense because of the slightly longer path the photons traverse before leaving the crystal. In the inset, the amplitude ratio for the central portion of the emission pattern is shown. The large values of about -50 at the emission peaks indicate, as mentioned earlier, that the emitted photon is mostly in the "diffracted" beam.

In Figs. 3 and 4, the number of photons per steradian emitted under those same conditions is displayed as a function of θ and ϕ for the θ and ϕ polarizations, respectively. It is the sum of these two contributions that resemble a cone.

Next we consider the dependence on the angle of incidence of the electron, θ_e. In Fig. 5, the peak of the ϕ polarization emission rate (photons per steradian per s), which occurs at the point labeled P_ϕ in Fig. 4, is plotted against θ_e for several electron energies. In Fig. 6, the same peak emission rate is shown plotted against the en-

ergy of the photon emitted at that point as θ_e is varied. Both these figures show how, as γ increases, the emission profile tends to saturate for lower angles or photon energies. Meanwhile, the maximum emission rate at $\gamma \hbar \omega_p$ moves towards higher photon energies; for diamond the plasma energy $\hbar \omega_p = 38.1$ eV leads to emission rate maxima at 7.62, 11.4, 19.0, 26.7, and 34.3 keV for $\gamma = 200$, 300, 500, 700, and 900, respectively. One sees that, as θ_e approaches 90°, the emission rate drops abruptly. As shown in Sec. III C, this is connected to the rapidly vanishing susceptibility.

Similar plots are shown in Figs. 7 and 8 for the peak number per steradian of ϕ-polarized photons which exit the crystal [this is given by Eq. (4.3) evaluated at P_ϕ] as a function of θ_e and of the emitted $\hbar \omega$. These figures are rather remarkable. Figure 7 clearly shows that, to generate DCR photons efficiently, high incidence angles are required but extreme grazing incidence should be avoided. Many of the experiments performed to date have looked for DCR photons at angles that are either too small or too large, which partly explains the rather poor quality of their results. In Fig. 8 we can see that, although the electron tends to emit most efficiently at the
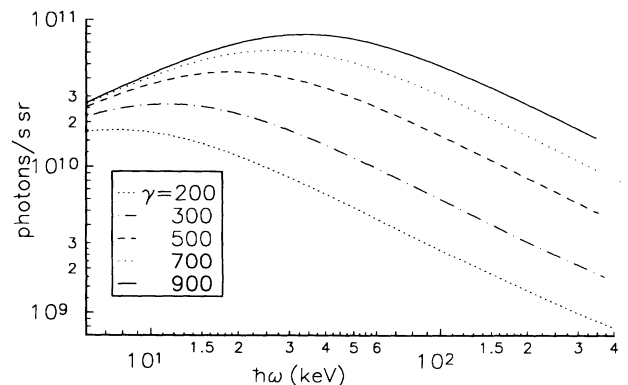

FIG. 4. The number of photons per steradian which exits the crystal as a function of the emission direction (ϕ polarization, $\gamma = 300$, $\theta_e = 85°$).

FIG. 6. The same ϕ-polarization peak emission rate of Fig. 5 is plotted against the energy of the photon emitted as θ_e is varied.
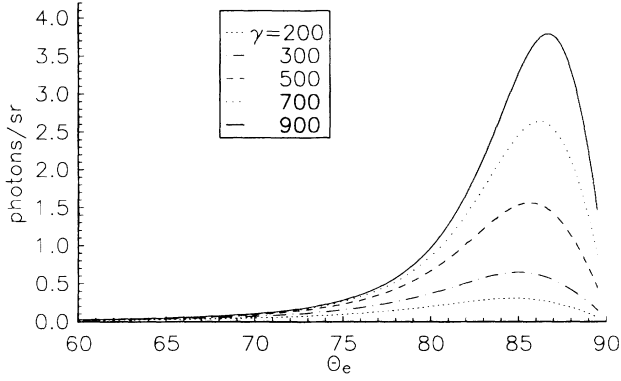
FIG. 7. The peak number per steradian of ϕ-polarized photons which exit the crystal [this is given by Eq. (4.3) evaluated at the point P_ϕ in Fig. 4] as a function of θ_e.

photon energy $\gamma \hbar \omega_p$, because of absorption the actual maximum of $dN/d\Omega$ is shifted to higher values of $\hbar \omega$ (of several tens of keV). In fact, since $dN/d\Omega$ decays rather slowly with the photon energy, we see that DCR is particularly efficient as a mechanism to generate very hard x rays.

The fact that the emission peak occurs at energies $\hbar \omega$ appreciably higher than $\gamma \hbar \omega_p$ implies that the actual values of the amplitude ratio $|R_c|$ selected by energy-momentum conservation in the region where DCR is large are appreciably larger than the minimum allowed. Using Eqs. (3.9), (3.10), and (3.17), the amplitude ratio R_c at the point P_ϕ (Fig. 4) is

$$R_c = -\left[1 + \left(\frac{\hbar \omega}{\gamma \hbar \omega_p} \right)^2 \right] \frac{2}{Pr_F} . \qquad (5.1)$$

In the region where DCR is large, because of absorption $\hbar \omega / \gamma \hbar \omega_p \approx 2-4$, putting $r_F = 0.36$ [diamond (111), a reasonably large value], we get $|R_c| \approx 25-90$.

Next we turn to the spectral density, given by Eq. (4.7), for varying electron incidence angle. In Fig. 9 the peak value of $d^2N/d\hbar \omega \, d\Omega$ [i.e., Eq. (4.7) evaluated at P_ϕ and at the energy $\hbar \omega$ that maximizes the Lorentzian in (4.7)]

FIG. 9. The peak value of $dN/d\hbar \omega \, d\Omega$ [i.e., Eq. (4.7) evaluated at the point P_ϕ in Fig. 4 and at the energy $\hbar \omega$ that maximizes the Lorentzian] is plotted against the emitted photon energy as θ_e is varied.

FIG. 10. The relative deviation of the photon energy ϵ_C from the Bragg-law prediction at the point P_ϕ, as a function of the electron angle of incidence θ_e.
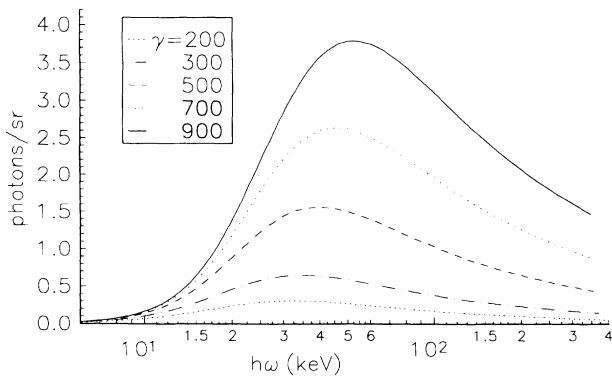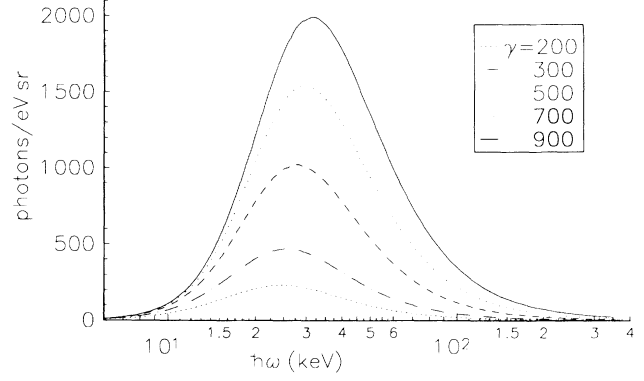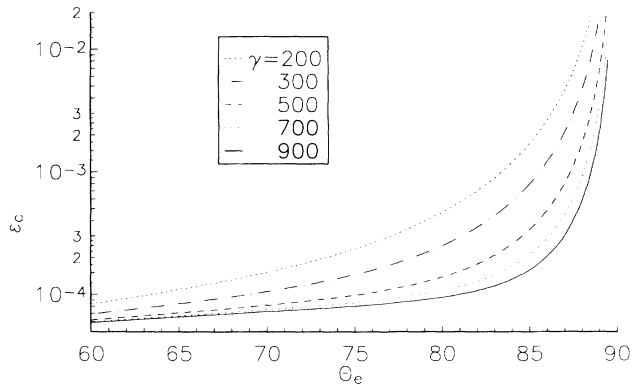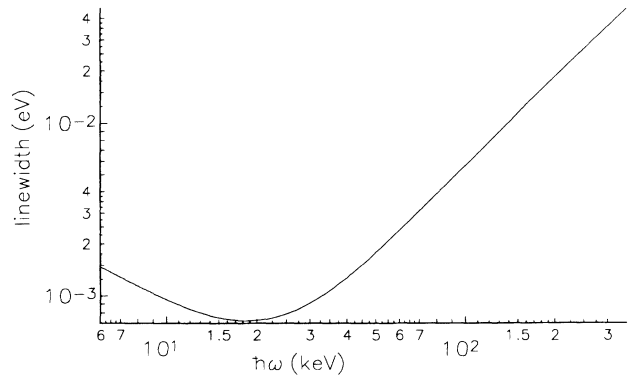

FIG. 8. The same peak number per steradian of ϕ-polarized photons which exit the crystal as in Fig. 7 as a function of the emitted $\hbar \omega$ as θ_e is varied.

FIG. 11. The spectral linewidth W due to x-ray absorption at the point P_ϕ as a function of the photon energy $\hbar \omega$ as θ_e is varied.

is plotted against the emitted photon energy as θ_e is varied. The most important feature of this graph is the sheer magnitude of the scale of the ordinate axis. It may be useful to compare with the synchrotron radiation spectral density obtainable from, say, a 4-GeV electron for a bending radius of 10 m: about 0.03 photons per eV per steradian at 35 keV. Since photon energies are strongly correlated to their direction of propagation, we conclude that very high spectral densities are possible provided the x-ray beam is sufficiently well collimated.

Finally, Figs. 10 and 11 show the systematic relative deviation of the photon energy ϵ_C from the Bragg-law prediction, and the spectral linewidth W due to x-ray absorption. Again, both graphs refer to the peak of ϕ polarization emission labeled P_ϕ in Fig. 4.

VI. CONCLUSIONS AND SOME FINAL COMMENTS

A quantum theory of DCR based on a phenomenological quantum electrodynamics has been given which is very closely related to the quantum theory of the Čerenkov effect. It can be shown that, in the limit in which electron recoil effects are neglected, this theory gives results which are identical to those of the classical theory.[6] The theory is simple enough to allow the calculation of the intrinsic spectral width, and of systematic deviations of the photon energy from Bragg's law, and of other features of the DCR process. Extensions of the theory to cover many-beam diffraction cases or more detailed calculations of the small recoil effects are straightforward to carry out.

The emitted photons have amplitude ratios which tend to be rather large, that is, the emission occurs at the far tails of the diffraction region. Thus, Bloch waves are overwhelmingly in the "diffracted" A_H plane-wave component, and, at least in the two-beam case DCR, there is no anomalous Borrmann absorption.

We have found that DCR is a particularly efficient emission process for hard x rays (several tens of keV) with a very high spectral density (within small angular regions). The emission rate is highest at the energy $\hbar\omega = \gamma\hbar\omega_p$ but, because of absorption, the number of photons which actually emerge from the crystal will peak at appreciably higher energies. The production of photons of a given energy is optimized by using lattice planes with the lowest possible Miller indices at the expense of having to go to more grazing incidence angles, and by asymmetrically cutting the crystal surface. This latter effect is actually to be expected given the existence of

similar effects in conventional x-ray diffraction.

The use of DCR for a tunable source of x rays should therefore be seriously considered. One important advantage of this x-ray production mechanism lies in the relatively low energy of the electron beam. This not only lowers the cost of the required equipment, but simplifies its manipulation. In particular, there is greater freedom in the temporal structure that may be imposed on such beams. This means that DCR x-ray pulses could, in principle, be much shorter than those obtained from storage rings. Thus, rather than competing with synchrotron radiation sources, DCR has the potential of becoming a *different* source, useful both for its efficiency in the harder part of the spectrum, for its very high spectral density, and for its possibly different temporal structure.

Further experimental work is necessary. The experiments performed to date have looked for DCR photons under unfavorable conditions. As mentioned earlier, in general, electron angles of incidence have been chosen which are either too small or too large. All of the experiments have had very low angular and spectral resolutions (none have employed crystal monochromators). Thus, one of the main features (high spectral density) distinguishing the DCR mechanism from other radiation mechanisms has not so far been fully exploited. Finally, all experiments have been carried out in the Laue-case geometry. This has the important drawback that the photons that reach the crystal surface are emitted by electrons that have already traversed some distance within the crystal with increased likelihood of multiple scatterings. In other words, Laue-case DCR photons are effectively generated by electron beams of poorer quality. One should expect that photons generated under Bragg-case conditions would exhibit the sharp features of the DCR process in a clearer way.

Finally, it is rather easy to obtain a lower bound for the threshold current density for stimulated DCR by totally neglecting stimulated absorption. We find that the threshold current must be larger than 10^9 A/cm^2, which is too high; it is very unlikely that an x-ray laser based on this process might work.

ACKNOWLEDGMENTS

---

*On leave from Instituto de Física "Gleb Wataghin," Universidade Estadual de Campinas, CP 6165, Campinas, S.P. 13081, Brazil.

[1] G. M. Garibyan and C. Yang, Zh. Eksp. Teor. Fiz. **61**, 930 (1971) [Sov. Phys. JETP **34**, 495 (1972)]; **63**, 1198 (1972) [**36**, 631 (1973)].

[2] V. G. Baryshevsky and I. D. Feranchuk, Zh. Eksp. Teor. Fiz. **61**, 944 (1971) [Sov. Phys. JETP **34**, 502 (1972)]; **64**, 760 (1973) [**37**, 760 (1973)].

[3] A. M. Afanas'ev and M. A. Aginyan, Zh. Eksp. Teor. Fiz. **74**, 570 (1978) [Sov. Phys. JETP **47**, 300 (1978)].

[4] See, e.g., B. Batterman and H. Cole, Rev. Mod. Phys. **36**, 681 (1964); N. Kato, in *X-Ray Diffraction*, edited by L. Azàroff (McGraw-Hill, New York, 1974), Chap. 4; Z. G. Pinsker, *Dynamical Scattering of X-Rays in Crystals* (Springer-Verlag, Berlin, 1978).

[5] V. G. Baryshevsky and I. D. Feranchuk, Dokl. Akad. Nauk B. SSR **18**, 499 (1974); Phys. Lett. **57A**, 183 (1976); J. Phys.

(Paris) **44**, 913 (1983).

[6]A. Caticha, Phys. Rev. A **40**, 4322 (1989).

[7]O. Brummer, H. Hoche, and J. Nieber, Phys. Status Solidi A **53**, 565 (1979).

[8]A. Caticha and S. Caticha-Ellis, Phys. Rev. B **25**, 971 (1982); Phys. Status Solidi A **119**, 47 (1990).

[9]V. G. Baryshevsky et al., J. Phys. D **19**, 171 (1986).

[10]Y. N. Adishchev et al., Zh. Eksp. Teor. Fiz. **90**, 829 (1986) [Sov. Phys. JETP **63**, 484 (1986)]; Nucl. Instrum. Methods B **21**, 49 (1987); Zh. Tekh. Fiz. **58**, 754 (1988) [Sov. Phys. Tech. Phys. **33**, 461 (1988)]; Nucl. Instrum. Methods B **44**, 130 (1989).

[11]R. O. Avakyan et al., Pis'ma Zh. Eksp. Teor. Fiz. **45**, 313 (1987) [JETP Lett. **45**, 396 (1987)].

[12]A. N. Didenko et al., Dokl. Akad. Nauk SSR **296**, 1360 (1987) [Sov. Phys. Dokl. **32**, 846 (1987)].

[13]D. I. Adeishvili et al., Dokl. Akad. Nauk SSSR **298**, 844 (1988) [Sov. Phys. Dokl. **33**, 117 (1988)].

[14]V. L. Ginzburg, J. Phys. (USSR) **2**, 441 (1940); J. M. Jauch and K. M. Watson, Phys. Rev. **74**, 950 (1948); **74**, 1485 (1948); J. A. Kong, Phys. Rev. D **12**, 3858 (1975).

[15]A. Caticha and N. Caticha (unpublished).

[16]A. Caticha, N. Caticha, and S. Caticha-Ellis, Appl. Phys. Lett. **54**, 887 (1989).

[17]See, e.g., J. D. Bjorken and S. D. Drell, *Relativistic Quantum Fields* (McGraw-Hill, New York, 1965); C. Itzykson and J. B. Zuber, *Quantum Field Theory* (McGraw-Hill, New York, 1980).

[18]I. Frank and I. Tamm, C. R. (Dokl.) Acad. Sci. URSS **14**, 109 (1937).

[19]R. T. Cox, Phys. Rev. **74**, 950 (1944).